JIR-2013-0124-ver9-Ceballos_1P
Type: research-article

FULL MANUSCRIPT

JOURNAL OF INTERFERON & CYTOKINE RESEARCH
Volume 00, Number 00, 2014

DOI: 10.1089/jir.2013.0124

AU1 ▶

FoxO3a Nuclear Localization and Its Association with β-Catenin and Smads in IFN-α-Treated Hepatocellular Carcinoma Cell Lines

AU2 ▶

María Paula Ceballos, Juan Pablo Parody, Ariel Darío Quiroga, María Laura Casella, Daniel Eleazar Francés, María Cecilia Larocca, Cristina Ester Carnovale, María de Luján Alvarez, and María Cristina Carrillo

Interferon-α2b (IFN-α2b) reduces proliferation and increases apoptosis in hepatocellular carcinoma cells by decreasing β-catenin/TCF4/Smads interaction. Forkhead box O-class 3a (FoxO3a) participates in proliferation and apoptosis and interacts with β-catenin and Smads. FoxO3a is inhibited by Akt, IκB kinase β (IKKβ), and extracellular-signal-regulated kinase (Erk), which promote FoxO3a sequestration in the cytosol, and accumulates in the nucleus upon phosphorylation by c-Jun N-terminal kinase (JNK) and p38 mitogen-activated kinase (p38 MAPK). We analyzed FoxO3a subcellular localization, the participating kinases, FoxO3a/β-catenin/Smads association, and FoxO3a target gene expression in IFN-α2b-stimulated HepG2/C3A and Huh7 cells. Total FoxO3a and Akt-phosphorylated FoxO3a levels decreased in the cytosol, whereas total FoxO3a levels increased in the nucleus upon IFN-α2b stimulus. IFN-α2b reduced Akt, IKKβ, and Erk activation, and increased JNK and p38 MAPK activation. p38 MAPK inhibition blocked IFN-α2b-induced FoxO3a nuclear localization. IFN-α2b enhanced FoxO3a association with β-catenin and Smad2/3/7. Two-step coimmunoprecipitation experiments suggest that these proteins coexist in the same complex. The expression of several FoxO3a target genes increased with IFN-α2b. FoxO3a knockdown prevented the induction of these genes, suggesting that FoxO3a acts as mediator of IFN-α2b action. Results suggest a β-catenin/Smads switch from TCF4 to FoxO3a. Such events would contribute to the IFN-α2b-mediated effects on cellular proliferation and apoptosis. These results demonstrate new mechanisms for IFN-α action, showing the importance of its application in antitumorigenic therapies.

Introduction

Forkhead box O-class (FoxO) transcription factors function as tumor suppressors (Greer and Brunet 2005) and both their expression and activity appear to be reduced in several tumor types (Maiese and others 2009; Yang and Hung 2011). In mammals, there are 4 members of the FoxO family: FoxO1 (FKHR), FoxO3a (FKHRL1), FoxO4 (AFX), and FoxO6 (Katoh and Katoh 2004). Functional activities of FoxOs are tightly regulated at post-translational level, mainly by reversible modifications such as phosphorylations. These events control FoxO subcellular localization and protein stability.

Among FoxO members, FoxO3a generates the most interest since it is a common target of protein kinase B or Akt, IκB kinase β (IKKβ), extracellular-signal-regulated kinase (Erk), c-Jun N-terminal kinase (JNK), and p38 mitogen-activated kinase (p38 MAPK) (Cai and Xia 2008; Yang and Hung 2011; Ho and others 2012). In response to growth factors or insulin stimulation, FoxO3a is negatively regulated by Akt, IKKβ, and Erk kinases (Greer and Brunet 2005; Yang and Hung 2011). Phosphorylation of FoxO3a by Akt (Thr32, Ser253, and Ser315), IKKβ (Ser644), and Erk (Ser294, Ser344, and Ser425) induces its nuclear exclusion and sequestration in the cytosol, thereby avoiding FoxO3a transcriptional activity (Brunet and others 1999; Hu and others 2004; Yang and others 2008). Once in the cytosol FoxO3a can undergo degradation through the ubiquitin-proteasome pathway (Yang and others 2008; Fu and others 2009; Tsai and others 2010). On the other hand, in response to several stress stimuli, FoxO3a is positively regulated by JNK and p38 MAPK leading to its nuclear localization and transcriptional activation (Brunet and others 2004; Ho and others 2012). While the JNK-phosphorylated FoxO3a residues are still unknown (Brunet and others 2004), p38 MAPK phosphorylates it at Ser7 (Ho and others 2012). In

Instituto de Fisiología Experimental, Consejo Nacional de Investigaciones Científicas y Técnicas (CONICET), Facultad de Ciencias Bioquímicas y Farmacéuticas, Universidad Nacional de Rosario, Rosario, Argentina.

the nucleus, FoxO3a binds to the DNA and modulates the transcription of different target genes. FoxO3a promotes apoptosis by inducing death cytokines, including the tumor necrosis factor-related apoptosis-inducing ligand (TRAIL) (Modur and others 2002). Additionally, FoxO3a plays a major role in cell cycle arrest by upregulating the cyclin-dependent kinase inhibitors $p27^{Kip1}$ (Medema and others 2000) and $p21^{Waf1/Cip1}$ (Seoane and others 2004).

FoxO3a interacts with other transcription factors, modifying its transcriptional activity and defining its regulated-target genes (Greer and Brunet 2005). In this regard, FoxO3a transcriptional activity is enhanced by its association with β-catenin and this interaction attenuates the oncogenic Wnt/β-catenin pathway (Essers and others 2005; Almeida and others 2007; Hoogeboom and others 2008). Similarly, FoxO3a associates with the TGF-β pathway intermediates Smads 2 and 3 proteins (Seoane and others 2004; Gomis and others 2006; Fu and Peng 2011). FoxO3a/β-catenin and FoxO3a/Smads participate in cell cycle arrest by enhancing the expression of $p27^{Kip1}$ (Essers and others 2005) and $p21^{Waf1/Cip1}$ (Seoane and others 2004), respectively.

Interferon-α (IFN-α) has been described as an essential cytokine for antiviral immunity with antiproliferative and immunomodulatory effects (Pfeffer 1997). Clinically, IFN-α has been used for the treatment of a number of solid tumors and hematological malignancies (Friedman 2008). In connection with this, IFN-α has also been used for delaying the progression of liver function impairment or for the prevention of hepatocellular carcinoma (HCC) development in patients with chronic hepatitis B or C (Kim and others 2011; Takeyasu and others 2012). Nowadays, some reports also suggest a potential efficacy of IFN-α therapy for HCC, either alone or in combination with other drugs (Shen and others 2010; Kasai and others 2012; Sakae and others 2012). In a previous work we have shown that IFN-α2b reduces the interaction of β-catenin and Smads with the TCF4 transcription factor, attenuating Wnt/β-catenin signal in 2 HCC cell lines. We demonstrated that the overall response to IFN-α2b was a decreased cellular proliferation and an increased apoptotic cell death (Ceballos and others 2011). Since FoxO3a associates with β-catenin and Smads and also participates in the apoptotic response and in the cell cycle arrest, we decided to explore whether FoxO3a signaling is involved in the IFN-α2b effects observed on HCC cell lines.

Materials and Methods

Reagents

IFN-α2b was kindly provided by PC-Gen (Buenos Aires, Argentina). Antibodies against p-Akt (Ser473), IKKβ, p-IKKβ (Ser177/181), Erk1/2 (against Erk 1 and 2 isoforms), p-Erk1/2 (Thr202/Tyr204), JNK1/2/3 (against JNK 1, 2, and 3 isoforms), and $p27^{Kip1}$ were purchased from Cell Signaling Technology (Danvers, MA). Anti-Histone H1, anti-Akt, anti-p-JNK1/2/3 (Thr183/Tyr185), anti-p38 MAPK, anti-p-p38 MAPK (Tyr182), anti-FoxO3a/FKHRL1, anti-p-FoxO3a/FKHRL1 (Ser253), anti-p-Smad2/3 (Ser433/435), anti-$p21^{Waf1/Cip1}$, and control immunoglobulin G (IgG) antibodies were from Santa Cruz Biotechnology, Inc. (Santa Cruz, CA). Anti-β-actin and anti-α-tubulin were from Sigma-Aldrich Corp. (St. Louis, MO). 4-(4-Fluorophenyl)-2-(4-hydroxyphenyl)-5-(4-pyridyl) 1H-imidazole (SB202190) was from Calbiochem (San Diego, CA). Anti-β-catenin antibody was from BD Transduction Labs (San Jose, CA). Antibody against TRAIL was obtained from Aviva Systems Biology (San Diego, CA). Anti-Smad7 antibody was obtained from R&D Systems (Minneapolis, MN). Phosphatases' inhibitor Calyculin A (PHZ1044) was from BioSource International (Camarillo, CA). All other chemicals were the highest grade commercially available.

Cell lines and treatments

The human HCC cell lines HepG2/C3A (a clonal derivative from HepG2) and Huh7 were obtained from American Type Culture Collection (Rockville, MD). Cells were maintained in Dulbecco's modified Eagle's medium supplemented with 10% fetal bovine serum, 100 IU/mL penicillin, and 100 μg/mL streptomycin at 37°C in a humidified atmosphere of 95% O_2 and 5% CO_2. Cells were plated with the maintenance medium and, the next day, they were starved by incubation in serum-free medium (SFM) for an hour at 37°C. SFM was composed of Iscove's modified Dulbecco's medium and F-12 Nutrient Mixture (Ham) (1:1), 20 IU/mL penicillin, 20 μg/mL streptomycin, and insulin-transferrin-selenium supplement (Gibco, Carlsbad, CA). After starvation, cells were treated for 48 h with 100,000 U/mL IFN-α2b or left untreated. During the experiments with p38 MAPK inhibitor, Huh7 cells were pretreated with 1 mM SB202190 for 1 h and then incubated for 48 h with or without 100,000 U/mL IFN-α2b, in the presence of the kinase inhibitor.

Preparation of total cell lysates and subcellular fractions

Cells were seeded in 10-cm plates at a density of 4×10^6 cells/plate for C3A and 2×10^6 cells/plate for Huh7. After treatments, total cell lysates and cytosolic and nuclear extracts were prepared as previously described (de Luján Alvarez and others 2004; Alvarez and others 2009). Total cell lysates used for coimmunoprecipitation experiments were obtained in nondenaturing lysis buffer containing 20 mM Tris (pH 8), 137 mM NaCl, 10% glycerol, 1% Triton X-100, 2 mM EDTA, 1 mM NaF, 1 mM Na_3VO_4, 1.5 nM Calyculin A, and protease inhibitors.

Protein concentration determination

The protein concentration was determined by the Lowry method (Lowry and others 1951), using bovine serum albumin as a standard.

Western blot analysis

Equal amounts of proteins were resolved by 12% sodium dodecyl sulfate–polyacrylamide gel electrophoresis (SDS-PAGE) and electroblotted onto polyvinyl difluoride (PVDF) membranes (PerkinElmer Life Sciences, Inc., Boston, MA). Immunoblots were blocked with PBS-10% nonfat milk, washed, and incubated overnight at 4°C with primary antibodies. Finally, membranes were incubated with peroxidase-conjugated secondary antibodies and bands were detected by enhanced chemiluminescence (ECL™) detection system (Thermo Fisher Scientific, Rockford, IL). The immunoreactive bands were quantified by densitometry using the Gel-Pro

Analyzer software (Media Cybernetics, Silver Spring, MD). Equal loading and protein transference were checked by detection of β-actin and Histone H1 for cytosolic and nuclear extracts, respectively, and double checked by Ponceau S staining of the membranes (latter data not shown). The purity of cytosolic and nuclear extracts was confirmed by immunoblot using α-tubulin and Histone H1 antibodies, as previously reported (Ceballos and others 2011) (data not shown).

Coimmunoprecipitation assays

Four hundred micrograms of total cell lysates was subjected to immunoprecipitation with 2 μg of specific primary antibodies or with control IgG for determining the specificity of the interaction. Proteins bound to Protein A-Sepharose® beads (Sigma-Aldrich Corp.) were washed and resolved by 10% SDS-PAGE. Gels were blotted onto PVDF membranes and incubated with specific primary and secondary antibodies at appropriate dilutions. The immunoreactive bands were detected as described previously.

For the 2-step coimmunoprecipitation assay, 800 μg of total cell lysates was subjected to a first immunoprecipitation with 4 μg of anti-p-Smad2/3 or anti-Smad7 antibodies or with control IgG. Immunocomplexes were isolated by bounding to Protein A-Sepharose® beads, washed, and divided into 2 equal fractions. One fraction was resolved by 10% SDS-PAGE and the other one was submitted to a second immunoprecipitation with 2 μg of anti-FoxO3a antibody or with control IgG. Finally, immunocomplexes were pulled down by bounding to magnetic Dynabeads® (Invitrogen, Carlsbad, CA), washed, and resolved by 10% SDS-PAGE. Then, protein samples from each step and aliquots of total cell lysates were subjected to western blot using anti-β-catenin and anti-FoxO3a antibodies.

FoxO3a expression reduction by short-interfering RNA

Four 21-nucleotide RNA duplexes [short-interfering RNA (siRNA)] targeting human FoxO3a mRNA were designed using the WIsiRNA selection program (Yuan and others 2004) and produced by Invitrogen. The control siRNA (scrambled) was designed by scrambling the nucleotides of one of these specific targets. The siRNAs were synthesized using the Silencer® siRNA Construction Kit (Ambion, Austin, TX).

Huh7 cells were seeded in 6-well plates at a density of 2.5×10^5 cells/well. On the following day, cells were transfected with 100 nM siRNAs using Lipofectamine 2000 (Invitrogen), according to the manufacturer's instructions. The specific decrease in FoxO3a protein expression was verified 24, 48, and 72 h afterward by western blot analysis in total cell lysates. Cells transfected with the second siRNA (siRNA2) consistently showed the lowest FoxO3a levels at all times, so we chose it for subsequent experiments. siRNA2 was specifically targeted to nucleotides 4729–4749 (AACCCTCCAATGTGTTTCAAC) of human FoxO3a. In the following experiments, cells were treated with 100,000 U/mL IFN-α2b or left untreated, 24 h after transfection. Finally, total RNA was extracted 48 h after IFN-α2b incubation.

RNA isolation, cDNA synthesis, and real-time quantitative polymerase chain reaction

Total RNA was isolated from HCC cell lines by the TriZOL method (Life Technologies, Inc., Gaithersburg, MD, USA) according to manufacturer's instructions. One microgram of total RNA was treated with DNase I (Thermo Fisher Scientific) and cDNA was made using an oligo-dT primer and M-MLV reverse transcriptase (Promega, Madison, WI, USA). Polymerase chain reaction (PCR) assay was performed using an Mx3000P Real-Time Thermocycler (Stratagene, La Jolla, CA) with SYBR Green I (Invitrogen). PCRs were initiated with incubation at 95°C for 2 min, followed by 40 cycles at 95°C for 15 s, 60°C for 30 s, and 72°C for 40 s. For each sample we analyzed cyclophillin A (*CYPA*) expression to normalize target gene expression. Primers were designed using Primer3 software (Rozen and Skaletsky 2000) and produced by Invitrogen. The list of genes with their primer sequences is given in Table 1. Gene-specific amplification ◀T1 was confirmed by a single peak in the melting curve analysis. Relative changes in gene expression were determined by using the $2^{-\Delta\Delta Ct}$ method (Schmittgen and Livak 2008).

Statistical analysis

Results were expressed as mean ± SE. Significance in differences was tested by Student's *t*-test. When comparisons were made between more than 2 experimental groups, significance in differences was tested by 1-way ANOVA, followed by Tukey's test. Differences were considered significant when the P value was < 0.05.

Results

IFN-α2b promotes FoxO3a nuclear localization without altering its expression

To evaluate the effect of IFN-α2b on FoxO3a expression and its subcellular localization, we first analyzed the mRNA levels of *FoxO3a* transcript by real-time quantitative PCR (q-PCR). FoxO3a gene expression did not change in IFN-α2b-stimulated cells (Fig. 1A). Then, FoxO3a protein levels ◀F1 were evaluated in total cell lysates and in cytosolic and

Table 1. Gene Identity, DNA Sequence, and Amplicon Size of Primers Used in Real-Time Quantitative Polymerase Chain Reaction

Gene	*Gene ID*	*Primer sequence 5′- 3′*	*Am (bp)*
FoxO3a	2309	F: GCATTGTGTGTGTTGCTTCC R: AAGCCACCTGAAATCACACC	97
TRAIL	8743	F: TGTTGGCACATGCCTGTAGT R: GCATGATCTCACCACACTGC	97
$p27^{Kip1}$	1027	F: GAGGTGCTTGGGAGTTTTGA R: TGTTTACACAGCCCGAAGTG	102
$p21^{Waf1/Cip1}$	1026	F: GATTAGCAGCGGAACAAGGA R: CAACTACTCCCAGCCCCATA	100
CYPA	5478	F: TCTGCCCACCTTAACAGACC R: AATTGCCCAACACACCAAAT	98

Am, amplicon size; bp, base pairs; F, forward primer; R, reverse primer; FoxO3a, forkhead box O-class 3a; TRAIL, tumor necrosis factor-related apoptosis-inducing ligand; CYPA, cyclophillin A.

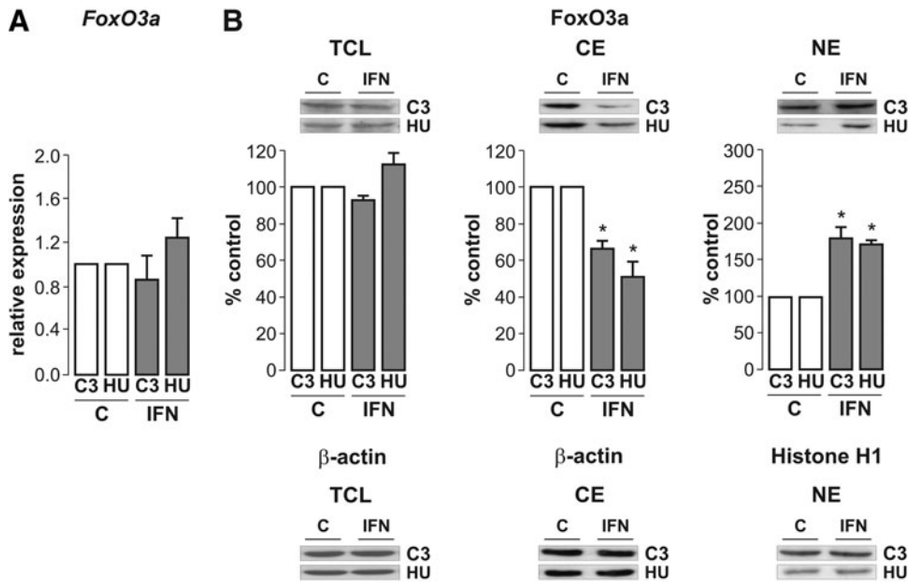

FIG. 1. Interferon-α2b (IFN-α2b) changes the subcellular localization of forkhead box O-class 3a (FoxO3a) but not its expression in hepatocellular carcinoma (HCC) cell lines. C3A and Huh7 cells were treated for 48 h in the presence or absence of IFN-α2b (100,000 U/mL). **(A)** Expression levels of the gene encoding FoxO3a (*FoxO3a*) were analyzed by real-time quantitative polymerase chain reaction (q-PCR). *FoxO3a* mRNA values in treated cells were calculated relative to the amount found in control cells, which was arbitrarily defined as 1. **(B)** Western blot analysis of FoxO3a protein levels was assessed in total cell lysates (TCL), cytosolic extracts (CE), and nuclear extracts (NE). β-Actin was detected as loading control for TCL and CE, whereas Histone H1 was probed as loading control for NE. Densitometric analysis was performed and results are expressed in percent values with control cells arbitrarily considered 100%. C: control (untreated) cells, IFN: cells treated with IFN-α2b, C3: C3A HCC cell line, HU: Huh7 HCC cell line. Mean ± SE; $n \geq 4$. *$P < 0.05$ versus C.

nuclear extracts from C3A and Huh7 cells by western blot. No changes were observed in FoxO3a levels in total cell lysates after IFN-α2b treatment (Fig. 1B). As seen in Fig. 1B, IFN-α2b stimulation led to a significant decrease in FoxO3a levels in cytosolic extracts (C3A: −34%; Huh7: −48%) that was correlated with a significant increase of this factor in nuclear extracts (C3A: +84%; Huh7: +72%).

IFN-α2b modulates Akt, IKKβ, Erk, JNK, and p38 MAPK

Phosphorylation of FoxO3a by Akt, IKKβ, and Erk kinases induces its sequestration in the cytosol, negatively regulating FoxO3a transcriptional activity. On the other hand, FoxO3a is positively regulated after being phosphorylated by JNK and p38 MAPK since these events lead to FoxO3a nuclear localization and transcriptional activation. To study the role of these kinases on the regulation of FoxO3a in IFN-α2b-treated cells, we analyzed the levels of the total and activated (phosphorylated) forms of each kinase in total cell lysates by western blot. As seen in Fig. 2, we found a significant diminution in the phosphorylated kinase/total kinase ratio for Akt, IKKβ, and Erk kinases in IFN-α2b-stimulated cells compared with control cells: p-Akt/Akt (C3A: −67%; Huh7: −61%), p-IKKβ/IKKβ (C3A: −22%; Huh7: −27%), and p-Erk/Erk (C3A: p-Erk1 −79%, p-Erk2 −56%; Huh7: p-Erk1 −46%, p-Erk2 −41%). On the other hand, there was a significant increase in p-JNK/JNK ratio (C3A: p-JNK2/3 +49%, p-JNK1 +64%; Huh7: p-JNK2/3 +45%, p-JNK1 +41%), as well as in p-p38 MAPK/p38 MAPK ratio (C3A: +96%; Huh7: +334%), in IFN-α2b-treated cells.

F2 ▶

IFN-α2b-induced FoxO3a nuclear localization depends on the phosphorylation status of Akt and p38 MAPK

To analyze whether Akt modulates FoxO3a in IFN-α2b-incubated cells, we examined the cytosolic protein levels of total FoxO3a and FoxO3a specifically phosphorylated by Akt at Ser253 (p-FoxO3a) by western blot. Figure 3 shows that p-FoxO3a/FoxO3a ratio significantly decreased in HCC cells treated with IFN-α2b (C3A: −36%; Huh7: −49%) compared with the ratio for control cells. This result is in line with the diminution observed in the p-Akt/Akt ratio in the presence of IFN-α2b.

◀ F3

So far, we found that IFN-α2b favored FoxO3a nuclear accumulation and p38 MAPK activation. Therefore, we decided to inhibit p38 MAPK with SB202190 in order to evaluate the potential role of p38 MAPK on FoxO3a nuclear accumulation upon IFN-α2b stimulus.

The SB202190 dose we used was the recommended in order to avoid nonspecific activity against other kinases (Bain and others 2007). SB202190 specificity was confirmed by assessing the phosphorylated kinase/total kinase ratio for Akt, IKKβ, Erk, and JNK kinases upon treatment with the inhibitor (data not shown).

Figure 4 shows the effect of IFN-α2b and SB202190 on p38 MAPK activation and subsequent action of p-p38 MAPK on FoxO3a nuclear localization. Figure 4A shows a significant increment in p-p38 MAPK/p38 MAPK ratio in IFN-α2b-stimulated cells compared with control cells (+334%). On the other hand, SB202190 was able to decrease basal p38 MAPK activation to a minimum (−82%).

◀ F4

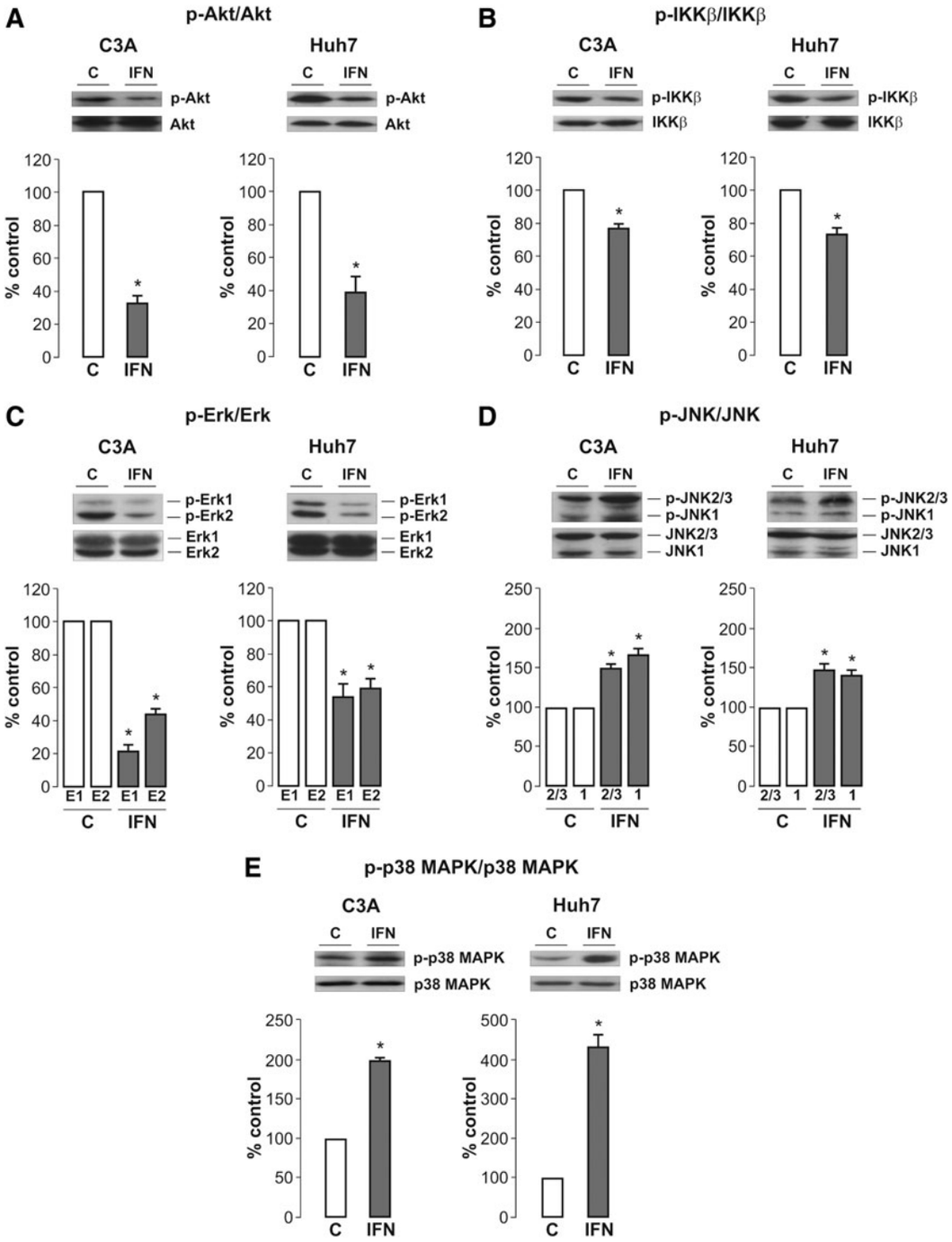

FIG. 2. Regulation of Akt, IκB kinase β (IKKβ), extracellular-signal-regulated kinase (Erk), c-Jun N-terminal kinase (JNK), and p38 mitogen-activated kinase (p38 MAPK) by IFN-α2b in HCC cell lines. C3A and Huh7 cells were incubated for 48 h in the presence or absence of IFN-α2b (100,000 U/mL). Levels of the phosphorylated and total forms of Akt **(A)**, IKKβ **(B)**, Erk **(C)**, JNK **(D)**, and p38 MAPK **(E)** were explored in TCL by western blot. The phosphorylated form of each protein was probed and then the total form was detected in the same membrane, after performing a stripping. Densitometric analysis was performed and results are expressed as the phosphorylated kinase/total kinase ratio and showed in percent values with control cells arbitrarily considered 100%. C: control (untreated) cells, IFN: cells treated with IFN-α2b, E1: p-Erk1, E2: p-Erk2, 2/3: p-JNK2/3, 1: p-JNK1. Mean ± SE; $n \geq 4$. *$P < 0.05$ versus C.

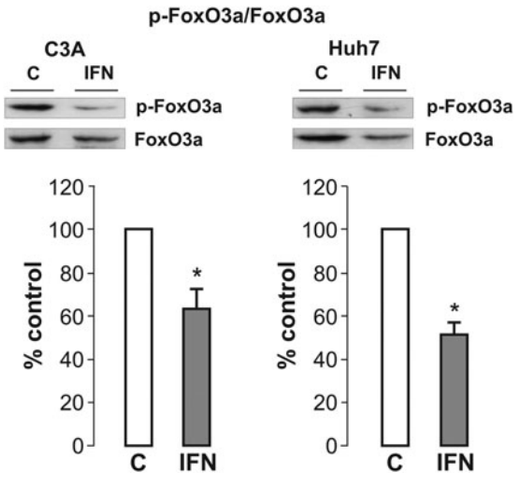

FIG. 3. IFN-α2b reduces Akt-phosphorylated FoxO3a levels in HCC cell lines. C3A and Huh7 cells were treated for 48 h in the presence or absence of IFN-α2b (100,000 U/mL). The amount of total FoxO3a and phosphorylated FoxO3a (p-FoxO3a) was evaluated by western blot in CE. Results are expressed as the p-FoxO3a/FoxO3a ratio. Phosphorylated FoxO3a was probed and then the total form of this protein was detected in the same membrane, after performing a stripping. Densitometric analysis was performed and results are expressed in percent values with control cells arbitrarily considered 100%. C: control (untreated) cells, IFN: cells treated with IFN-α2b. Mean ± SE; $n \geq 4$. $^{*}P < 0.05$ versus C; $^{\#}P < 0.05$ versus IFN.

However, the addition of IFN-α2b was able to reverse the inhibition of p38 MAPK, since it produced a significant raise of the p-p38 MAPK/p38 MAPK ratio (+142%) compared with control cells. This ratio, however, was significantly lower (−191%) than the ratio found in the presence of IFN-α2b alone. These results suggest that even in the presence of p38 MAPK inhibitor, IFN-α2b can induce p38 MAPK phosphorylation by a mechanism that needs to be elucidated.

Figure 4B shows that neither IFN-α2b nor SB202190 or their combination changed FoxO3a levels in total cell lysates. On the other hand, Fig. 4C shows that p38 MAPK inhibition resulted in a significant increment of cytosolic FoxO3a protein levels (+39%) and a decrease of nuclear FoxO3a protein levels (−57%), compared with those for control cells. When cells were stimulated with IFN-α2b in the presence of SB202190, we observed a significant decrease in cytosolic FoxO3a protein levels (−26%) compared with control cells. In addition, although we found a significant increase in nuclear FoxO3a protein levels (+31%) compared with control cells, this level was significantly lower (−40%) compared with the levels found in the presence of IFN-α2b alone. In addition, we calculated the FoxO3a nuclear/cytosolic ratio and we observed that it increased with IFN-α2b and diminished in the presence of SB202190, compared with control cells. Also, we found an increment in this ratio when cells were stimulated with IFN-α2b in the presence of SB202190, being this level significantly lower compared with the levels found in the presence of IFN-α2b alone. Therefore, SB202190 partially prevented the increment in nuclear FoxO3a seen in IFN-α2b-treated HCC cells. These results indicate that p38 MAPK mediates FoxO3a nuclear localization, since its inhibition blocked both constitutive and cytokine-induced FoxO3a nuclear accumulation.

Given that JNK activation by IFN-α2b also induced the increment of nuclear FoxO3a, we attempted to inhibit this kinase with the JNK inhibitor SP600125. Unfortunately, we could not arrive at a conclusive result because SP600125 inhibited some of the other kinases under study (data not shown). Previous reports informed that SP600125 was a relatively weak inhibitor of JNK isoforms and that other protein kinases were inhibited with similar or greater potency by SP600125 (Bain and others 2003, 2007).

IFN-α2b stimulates FoxO3a interaction with β-catenin and Smads 2 and 3

C3A and Huh7 cells were stimulated with IFN-α2b and then coimmunoprecipitation experiments were performed using total cell lysates. IFN-α2b favored FoxO3a association with β-catenin and Smad2/3 (Fig. 5A). To examine whether FoxO3a, β-catenin, and Smad2/3 are forming a tripartite complex, cells were treated with IFN-α2b and 2-step co-immunoprecipitation experiments were carried out. As shown in Fig. 5B, β-catenin was detected in the final immunoprecipitate, suggesting that Smad2/3, FoxO3a, and β-catenin coexist in the same complex. ◀F5

IFN-α2b enhances the expression of FoxO3a target genes

We analyzed the mRNA and protein levels of some FoxO3a target genes after IFN-α2b treatment. We chose some genes that are induced when FoxO3a binds alone to its target promoters such as in TRAIL or by forming a complex with β-catenin or Smad2/3 such as in $p27^{Kip1}$ or $p21^{Waf1/Cip1}$, respectively. IFN-α2b not only induced the expression of *TRAIL*, $p27^{Kip1}$, and $p21^{Waf1/Cip1}$ mRNAs (Fig. 6A), but also generated a significant increment in TRAIL (C3A: +120%; Huh7: +51%), $p27^{Kip1}$ (C3A: +66%; Huh7: +70%), and $p21^{Waf1/Cip1}$ (C3A: +69%; Huh7: +57%) protein levels in both HCC cell lines (Fig. 6B). ◀F6

To elucidate whether FoxO3a mediates *TRAIL*, $p27^{Kip1}$, and $p21^{Waf1/Cip1}$ mRNA induction in IFN-α2b-treated cells, its expression was knocked down with specific siRNAs. Four different siRNAs were tested in Huh7 cells and FoxO3a expression was checked 24, 48, and 72 h later by western blot. Among these, the siRNA2 induced a significant decrease in FoxO3a expression at all studied times (Fig. 7A) and it was chosen for the evaluation of FoxO3a target gene expression. The densitometric analysis relating FoxO3a to β-actin levels showed a decrease in FoxO3a expression of −64%, −46%, and −52% in siRNA2-treated cells at 24, 48, and 72 h, respectively (data not shown). ◀F7

Figure 7B shows the analysis of FoxO3a target gene expression using the siRNA2 or scrambled siRNA. Cells transfected with scrambled siRNA exhibited the induction of *TRAIL*, $p27^{Kip1}$, and $p21^{Waf1/Cip1}$ mRNAs by IFN-α2b, similar to that previously observed in wild-type cells. On the other hand, the siRNA2 completely abolished the IFN-α2b-mediated induction of these mRNAs, strongly suggesting that FoxO3a is indeed implicated in the regulation of *TRAIL*, $p27^{Kip1}$, and $p21^{Waf1/Cip1}$ expression by IFN-α2b.

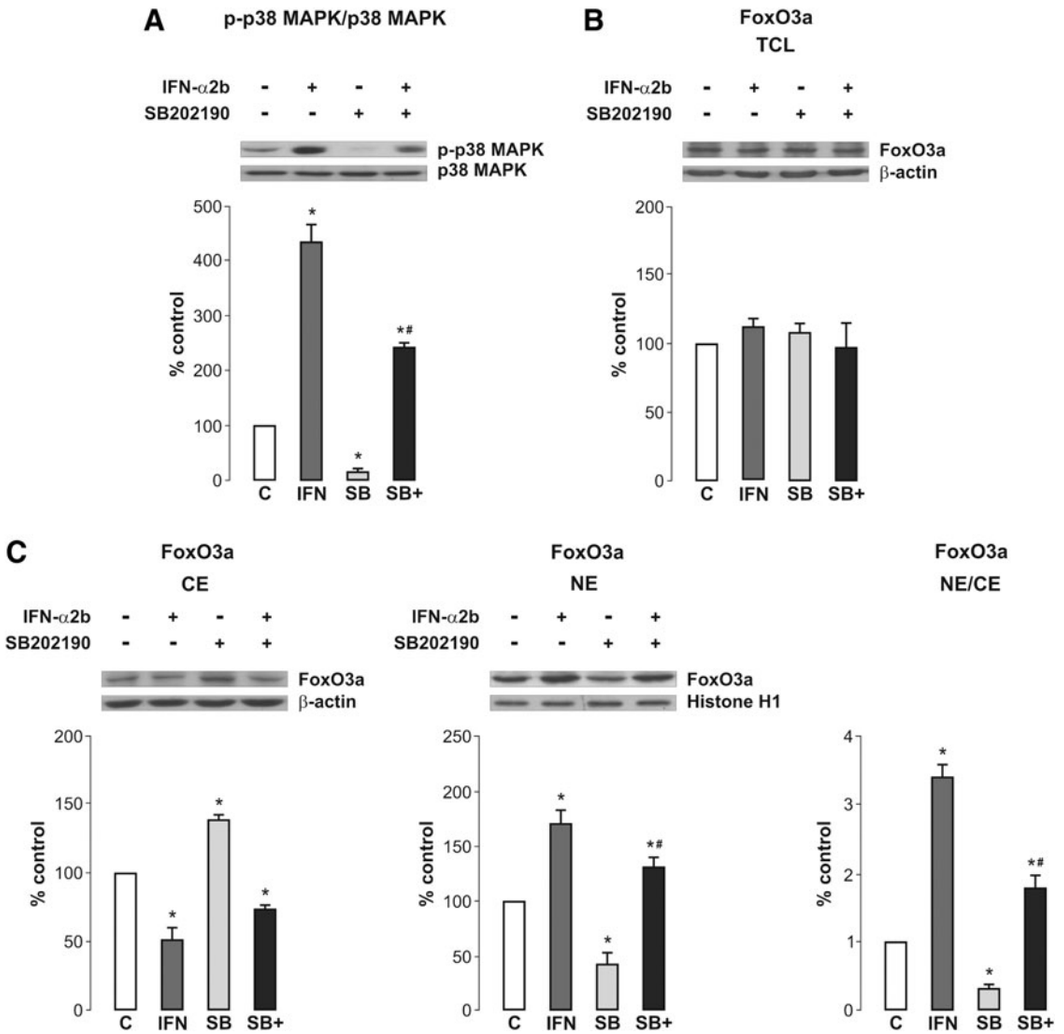

FIG. 4. p38 MAPK mediates IFN-α2b-induced FoxO3a nuclear localization in HCC cell lines. Huh7 cells were incubated in the presence or absence of SB202190 inhibitor (1 mM) for 1 h prior to IFN-α2b (100,000 U/mL) treatment. **(A)** The levels of the phosphorylated and total forms of p38 MAPK were measured in TCL by western blot. Results are expressed as the p-p38 MAPK/p38 MAPK ratio. The phosphorylated form of p38 MAPK was probed and then the total form of this protein was detected in the same membrane, after performing a stripping. **(B, C)** FoxO3a protein levels were measured in TCL, CE, and NE by western blot. β-Actin was detected as loading control for TCL and CE, whereas Histone H1 was probed as loading control for NE. The results were also expressed as the ratio of cytosolic-to-nuclear FoxO3a. Densitometric analyses were performed and results are expressed in percent values with control cells arbitrarily considered 100%. C: control (untreated) cells, SB: cells incubated with SB202190, IFN: cells treated with IFN-α2b, SB+: cells treated with SB202190 and then incubated with IFN-α2b. Mean ± SE; $n \geq 4$. $^{*}P < 0.05$ versus C; $^{\#}P < 0.05$ versus IFN.

IFN-α2b stimulates Smad7 association with FoxO3a and β-catenin

Finally, since Smad7 protein is able to interact with β-catenin, we analyzed whether Smad7 was also able to interact with FoxO3a in Huh7 cells. As seen in Fig. 8A, Smad7 interacted with FoxO3a, and interestingly, IFN-α2b enhanced their association. We also performed 2-step coimmunoprecipitation experiments in Huh7 cells to determine whether Smad7 integrates a ternary complex with FoxO3a and β-catenin. As shown in Fig. 8B, β-catenin was immunodetected after the second immunoprecipitation step, indicating that these proteins probably exist as a Smad7/FoxO3a/β-catenin ternary complex in IFN-α2b-treated cells.

F8 ▶

Discussion

It is important to understand the mechanisms underlying inhibition of growth and induction of apoptosis in cancer cells. In this connection, IFN-α exerts antiproliferative and proapoptotic activities (Friedman 2008); however, the mechanisms involved in these actions are not fully understood.

This is the first study that addresses the actions of IFN-α on FoxO3a signaling in HCC cell lines. We centered our research in 4 key cellular processes: (1) the effect of IFN-α on the regulation and subcellular localization of FoxO3a, (2) the kinases involved in this process, (3) the association of FoxO3a with β-catenin and Smads, and (4) the expression of some FoxO3a target genes in HepG2/C3A and Huh7 HCC cell lines.

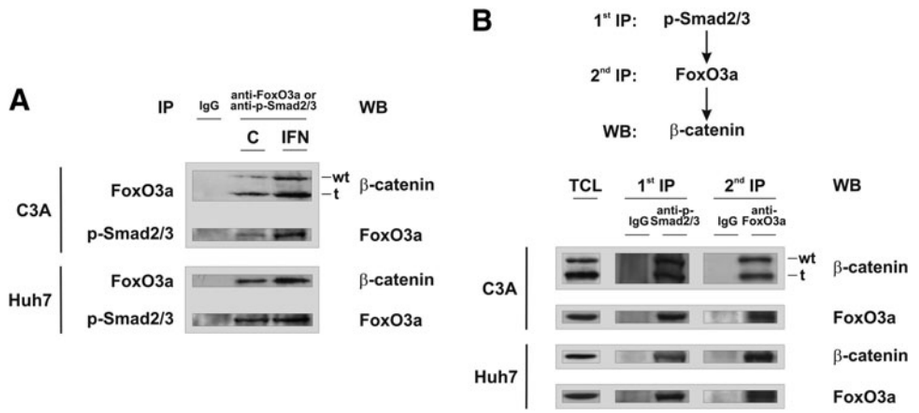

FIG. 5. I@FN-α2b-enhanced FoxO3a association with β-catenin and Smad2/3 in HCC cell lines. C3A and Huh7 cells were treated for 48 h in the presence or absence of IFN-α2b (100,000 U/mL) **(A)** or only with IFN-α2b **(B)**. Proteins from TCL were immunoprecipitated (IP) with specific antibodies or with control immunoglobulin G (IgG) and were analyzed by western blot (WB). **(A)** Coimmunoprecipitation experiment. IP was made with anti-FoxO3a and anti-p-Smad2/3 antibodies or with control IgG. β-Catenin and FoxO3a were detected by WB. **(B)** Two-step coimmunoprecipitation experiment. The procedure is outlined on the top of the figure. The first immunoprecipitation (1st IP) was performed with anti-p-Smad2/3 antibody or with control IgG and the second immunoprecipitation (2nd IP) with anti-FoxO3a antibody or with control IgG. Protein samples from each step were subjected to WB using anti-FoxO3a and anti-β-catenin antibodies. C: control (untreated) cells, IFN: cells treated with IFN-α2b, wt: wild-type β-catenin, t: truncated β-catenin, TCL: total cell lysates.

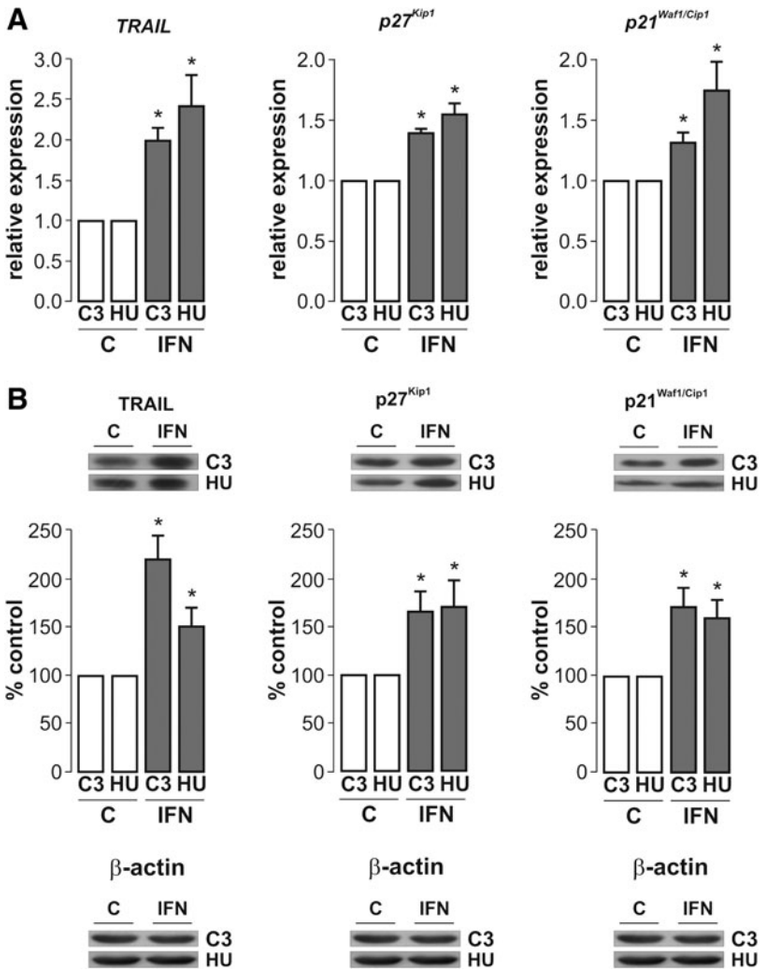

FIG. 6. Induction of FoxO3a target genes by IFN-α2b in HCC cell lines. C3A and Huh7 cells were treated for 48 h in the presence or absence of IFN-α2b (100,000 U/mL). **(A)** Expression levels of the genes encoding tumor necrosis factor-related apoptosis-inducing ligand (*TRAIL*), $p27^{Kip1}$ (*$p27^{Kip1}$*), and $p21^{Waf1/Cip1}$ (*$p21^{Waf1/Cip1}$*) were analyzed by real-time q-PCR. mRNA values in treated cells were calculated relative to the amount found in untreated cells, which was arbitrarily defined as 1. **(B)** Western blot analysis of TRAIL, $p27^{Kip1}$, and $p21^{Waf1/Cip1}$ protein levels was assessed in TCL. β-Actin was detected as loading control. Densitometric analysis was performed and results are expressed in percent values with control cells arbitrarily considered 100%. C: control (untreated) cells, IFN: cells treated with IFN-α2b, C3: C3A HCC cell line, HU: Huh7 HCC cell line. Mean ± SE; $n \geq 4$. *$P < 0.05$ versus C.

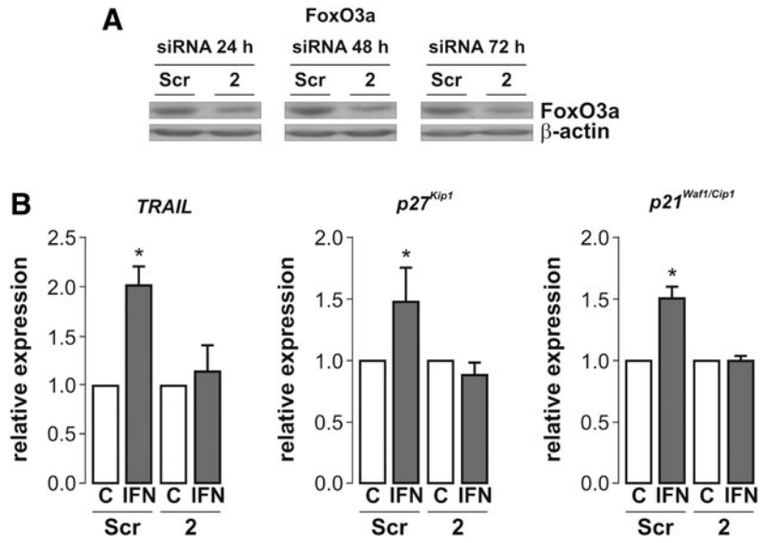

FIG. 7. FoxO3a mediates the induction of its target genes in IFN-α2b-treated HCC cell lines. Huh7 cells were transfected either with 100 nM scrambled short-interfering RNA (siRNA) (Scr) or with 100 nM siRNA2 (2) targeting human FoxO3a mRNA. **(A)** Representative western blot images for FoxO3a in TCL at 24, 48, and 72 h post-transfection, with β-actin as loading controls. **(B)** Twenty-four hours after transfection, cells were treated for 48 h in the presence or absence of IFN-α2b (100,000 U/mL). Expression levels of the genes encoding TRAIL (*TRAIL*), $p27^{Kip1}$ (*$p27^{Kip1}$*), and $p21^{Waf1/Cip1}$ (*$p21^{Waf1/Cip1}$*) were analyzed by real-time q-PCR. mRNA values in treated cells were calculated relative to the amount found in untreated cells, which was arbitrarily defined as 1. C: control (untreated) cells, IFN: cells treated with IFN-α2b. Mean ± SE; $n \geq 4$. *$P < 0.05$ versus C.

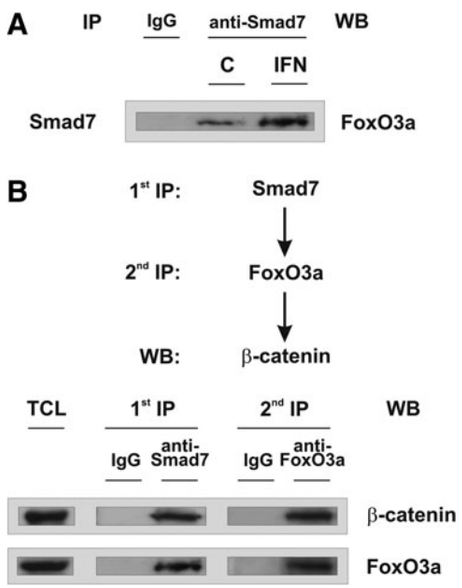

FIG. 8. IFN-α2b-promoted interaction of Smad7 with FoxO3a and β-catenin in HCC cell lines. Huh7 cells were treated for 48 h in the presence or absence of IFN-α2b (100,000 U/mL) **(A)** or only with IFN-α2b **(B)**. **(A)** Coimmunoprecipitation experiment. Proteins from TCL were immunoprecipitated (IP) with anti-Smad7 antibody or with control IgG (IgG) and were analyzed by western blot (WB) using anti-FoxO3a antibody. **(B)** Two-step coimmunoprecipitation experiment. The procedure is outlined on the top of the figure. The first immunoprecipitation (1st IP) was performed with anti-Smad7 antibody or with control IgG using TCL and the second immunoprecipitation (2nd IP) with anti-FoxO3a antibody or with control IgG. Protein samples from each step were then subjected to WB using anti-FoxO3a and anti-β-catenin antibodies. C: control (untreated) cells, IFN: cells treated with IFN-α2b, TCL: total cell lysates.

It is well known that FoxO3a transcription factor participates in proliferative and apoptotic events (Greer and Brunet 2005). Akt, IKKβ, and Erk, negative regulators of FoxO3a, are commonly activated in HCC and other tumor types (Cervello and others 2012). It has been reported in human tumors and tumor cell lines that phosphorylation and inactivation of FoxO3a by these oncogenic kinases favors cell transformation, proliferation, and survival (Brunet and others 1999; Hu and others 2004; Greer and Brunet 2005). However, it was also demonstrated that activation of FoxO3a signaling leads to cell cycle arrest and/or apoptosis (Modur and others 2002; Yang and Hung 2011; Ho and others 2012). Taken together, these evidences support the notion that FoxO3a may be acting as a tumor suppressor.

Our present results show that there is a cytosol-to-nucleus translocation of FoxO3a under IFN-α2b stimulus. In addition, we show that IFN-α2b stimulation induces a reduction in the activation of the protein kinases that inhibit FoxO3a and an increment in the activation of JNK and p38 MAPK that activate this factor. The modulation of Akt, Erk, JNK, and p38 MAPK by IFN-α was already reported in HCC (Inamura and others 2005; Zhou and others 2007; Franceschini and others 2011; Zhao and others 2011) and other cell types (Li and others 2004; Quiroga and others 2009; Dal Col and others 2012; Yanase and others 2012); however, there are no studies on the effects of IFN-α on IKKβ phosphorylation status in HCC or other cell types.

Akt-dependent phosphorylation on Ser253 abolishes FoxO3a nuclear translocation (Brunet and others 1999). Here, we report that IFN-α2b reduces Akt activation and FoxO3a phosphorylation, suggesting that IFN-α2b-induced attenuation of Akt activation is involved on the cellular fate of FoxO3a when incubated with IFN-α2b.

On the other hand, p38 MAPK inhibition largely abolishes nuclear accumulation of FoxO3a. This result confirms that p38 MAPK activation is necessary for FoxO3a nuclear translocation, as previously demonstrated (Cai and Xia 2008; Ho and others 2012). In addition, the inhibition of p38 MAPK significantly reverses IFN-α2b-induced FoxO3a nuclear accumulation. Since we found substantial p38 MAPK activation upon IFN-α2b stimulus, we inferred that

p38 MAPK mediates the nuclear accumulation of FoxO3a triggered by IFN-α2b.

Taken together, our findings indicate that p38 MAPK activation and Akt deactivation play crucial roles in IFN-α2b signaling to favor FoxO3a nuclear localization. Nevertheless, we cannot discard the involvement of other kinases (like IKKβ, Erk, and JNK) in IFN-α2b-mediated FoxO3a subcellular localization, since the final balance between the kinases that positively and negatively regulate FoxO3a will determine the ultimate nuclear amount of this transcription factor.

We previously described a diminution in the nuclear levels of β-catenin and Smad2/3 proteins and a reduction in the binding of these proteins to TCF4 in IFN-α2b-stimulated C3A and Huh7 cells (Ceballos and others 2011). In the present study we show that IFN-α2b favors FoxO3a interaction with β-catenin and Smad2/3, by probably cooperating simultaneously in a single nuclear complex. However, we cannot discard the scenario in which FoxO3a is interacting with β-catenin or Smad2/3 separately in IFN-α2b-treated HCC cell lines. To our knowledge, this is the first report that has started to explore these alternatives.

Altogether, our results suggest (1) that FoxO3a interaction with β-catenin and Smad2/3 is prompted in the presence of low levels of the latter proteins and high levels of FoxO3a, and (2) a switch of β-catenin and Smad2/3 association from TCF4 to FoxO3a induced by IFN-α2b. Preceding studies showed that FoxO3a and TCF4 compete for a limited pool of nuclear β-catenin and that FoxO3a overexpression is sufficient to reduce TCF4/β-catenin binding and to elevate FoxO3a/β-catenin association (Almeida and others 2007; Hoogeboom and others 2008). In agreement with our results, Kwon and others (2010) reported that diminutions in β-catenin levels and increments in FoxO levels lead to β-catenin sequestration by FoxO and inhibition of TCF-dependent transcription in colon cancer cells.

Taken together our results and others, it can be outlined a model in which IFN-α2b inhibits the formation of β-catenin/TCF4/Smad2/3 complex by 2 different ways: one is by reducing the amount of nuclear β-catenin and Smad2/3, and another is by activating FoxO3a, which ultimately binds to β-catenin and Smad2/3 limiting the available pool to interact with TCF4.

Once in the nucleus, FoxO3a is transcriptionally active and modulates a set of target genes. Here, we report that IFN-α2b induces an increment in the expression of the evaluated FoxO3a target genes. In addition, FoxO3a knockdown prevented the effect of IFN-α2b on these genes, strongly suggesting that FoxO3a mediates the IFN-α2b response. Expression of $p27^{Kip1}$ and $p21^{Waf1/Cip1}$ occurs as a consequence of FoxO3a/β-catenin and FoxO3a/Smad2/3 complex formation, respectively; therefore, these results are consistent with the enhanced interaction of these proteins in the presence of IFN-α2b. TRAIL is implicated in apoptosis (Wiley and others 1995), whereas $p27^{Kip1}$ and $p21^{Waf1/Cip1}$ are involved in cell cycle arrest (Harper and others 1993; Toyoshima and Hunter 1994), so the diminution in cellular proliferation and the increment in apoptosis generated by IFN-α2b (Ceballos and others 2011) would be related to the attenuation of Wnt/β-catenin pathway and the enhancement of FoxO3a signal. Indeed, TRAIL was identified as an important mediator of IFN-α2b-induced apoptosis in hepatoma cells (Herzer and others 2009) and other cell types (Kayagaki and others 1999; Papageorgiou and others 2007). In addition, it was demonstrated that IFN-α was able to modulate cell proliferation by inducing the expression of $p27^{Kip1}$ (Zhou and others 1999; Moro and others 2000) and $p21^{Waf1/Cip1}$ (Legrand and others 2004; Katayama and others 2007). All these data suggest that FoxO3a is acting as a molecular mediator of IFN-α2b-induced cellular arrest and apoptosis through activation of its downstream targets.

Finally, we wanted to investigate whether Smad7 interacted with FoxO3a as well. Results from coimmunoprecipitation experiments reveal that Smad7 associates with FoxO3a upon IFN-α2b treatment in Huh7 cells. It is likely that these proteins are part of a ternary complex together with β-catenin. To the best of our knowledge, this is the first study that describes a link between Smad7 and FoxO factors. Since we previously described a diminution in the Smad7/TCF4 binding in C3A and Huh7 cells stimulated with IFN-α2b (Ceballos and others 2011), these results suggest a switch of Smad7 association from TCF4 to FoxO3a that goes along with that of β-catenin and Smad2/3.

In conclusion, IFN-α2b arises as an attractive tool to evaluate the events of inhibition of growth and induction of apoptosis in cancer cells. In addition, these results support the use of IFN-α2b for the treatment of HCC. The results presented in this work not only show that IFN-α2b generates the binding switch of β-catenin and Smads from TCF4 to FoxO3a (attenuating Wnt/β-catenin pathway and promoting FoxO3a signaling), but they also demonstrate that IFN-α2b acts as a negative modulator of the oncogenic kinases Akt, IKKβ, and Erk. The elucidation of the signals induced by IFN-α in human liver malignancies paves the way for future design of specific therapeutic strategies in order to balance the cellular responses to favor liver tumor suppression.

Acknowledgments

This work was supported by research grants PIP 1246 (MC Carrillo) from Consejo Nacional de Investigaciones Científicas y Técnicas (CONICET) and by Instituto Nacional del Cáncer (INC, Ministerio de Salud de la Nación).

Author Disclosure Statement

No competing financial interests exist.

References

Almeida M, Han L, Martin-Millan M, O'Brien CA, Manolagas SC. 2007. Oxidative stress antagonizes Wnt signaling in osteoblast precursors by diverting beta-catenin from T cell factor- to forkhead box O-mediated transcription. J Biol Chem 282:27298–27305.

Alvarez Mde L, Quiroga AD, Parody JP, Ronco MT, Francés DE, Carnovale CE, Carrillo MC. 2009. Cross-talk between IFN-alpha and TGF-beta1 signaling pathways in preneoplastic rat liver. Growth Factors 27:1–11.

Bain J, McLauchlan H, Elliott M, Cohen P. 2003. The specificities of protein kinase inhibitors: an update. Biochem J 371:199–204.

Bain J, Plater L, Elliott M, Shpiro N, Hastie CJ, McLauchlan H, Klevernic I, Arthur JS, Alessi DR, Cohen P. 2007. The selectivity of protein kinase inhibitors: a further update. Biochem J 408:297–315.

Brunet A, Bonni A, Zigmond MJ, Lin MZ, Juo P, Hu LS, Anderson MJ, Arden KC, Blenis J, Greenberg ME. 1999. Akt promotes cell survival by phosphorylating and inhibiting a Forkhead transcription factor. Cell 96:857–868.

Brunet A, Sweeney LB, Sturgill JF, Chua KF, Greer PL, Lin Y, Tran H, Ross SE, Mostoslavsky R, Cohen HY, Hu LS, Cheng HL, Jedrychowski MP, Gygi SP, Sinclair DA, Alt FW, Greenberg ME. 2004. Stress-dependent regulation of FOXO transcription factors by the SIRT1 deacetylase. Science 303:2011–2015.

Cai B, Xia Z. 2008. p38 MAP kinase mediates arsenite-induced apoptosis through FOXO3a activation and induction of Bim transcription. Apoptosis 13:803–810.

Ceballos MP, Parody JP, Alvarez Mde L, Ingaramo PI, Carnovale CE, Carrillo MC. 2011. Interferon-α2b and transforming growth factor-β1 treatments on HCC cell lines: are Wnt/β-catenin pathway and Smads signaling connected in hepatocellular carcinoma? Biochem Pharmacol 82:1682–1691.

Cervello M, McCubrey JA, Cusimano A, Lampiasi N, Azzolina A, Montalto G. 2012. Targeted therapy for hepatocellular carcinoma: novel agents on the horizon. Oncotarget 3:236–260.

Dal Col J, Mastorci K, Faè DA, Muraro E, Martorelli D, Inghirami G, Dolcetti R. 2012. Retinoic acid/alpha-interferon combination inhibits growth and promotes apoptosis in mantle cell lymphoma through Akt-dependent modulation of critical targets. Cancer Res 72:1825–1835.

de Luján Alvarez M, Ronco MT, Ochoa JE, Monti JA, Carnovale CE, Pisani GB, Lugano MC, Carrillo MC. 2004. Interferon alpha-induced apoptosis on rat preneoplastic liver is mediated by hepatocytic transforming growth factor beta(1). Hepatology 40:394–402.

Essers MAG, de Vries-Smits LM, Barker N, Polderman PE, Burgering BM, Korswagen HC. 2005. Functional interaction between beta-catenin and FOXO in oxidative stress signaling. Science 308:1181–1184.

Franceschini L, Realdon S, Marcolongo M, Mirandola S, Bortoletto G, Alberti A. 2011. Reciprocal interference between insulin and interferon-alpha signaling in hepatic cells: a vicious circle of clinical significance? Hepatology 54:484–494.

Friedman RM. 2008. Clinical uses of interferons. Br J Clin Pharmacol 65:158–162.

Fu G, Peng C. 2011. Nodal enhances the activity of FoxO3a and its synergistic interaction with Smads to regulate cyclin G2 transcription in ovarian cancer cells. Oncogene 30:3953–3966.

Fu W, Ma Q, Chen L, Li P, Zhang M, Ramamoorthy S, Nawaz Z, Shimojima T, Wang H, Yang Y, Shen Z, Zhang Y, Zhang X, Nicosia SV, Zhang Y, Pledger JW, Chen J, Bai W. 2009. MDM2 acts downstream of p53 as an E3 ligase to promote FOXO ubiquitination and degradation. J Biol Chem 284: 13987–14000.

Greer E, Brunet A. 2005. FOXO transcription factors at the interface between longevity and tumor suppression. Oncogene 24:7410–7425.

Gomis RR, Alarcón C, Nadal C, Van Poznak C, Massagué J. 2006. C/EBPbeta at the core of the TGFbeta cytostatic response and its evasion in metastatic breast cancer cells. Cancer Cell 10:203–214.

Harper JW, Adami GR, Wei N, Keyomarsi K, Elledge SJ. 1993. The p21 Cdk-interacting protein Cip1 is a potent inhibitor of G1 cyclin-dependent kinases. Cell 75:805–816.

Herzer K, Hofmann TG, Teufel A, Schimanski CC, Moehler M, Kanzler S, Schulze-Bergkamen H, Galle PR. 2009. IFN-alpha-induced apoptosis in hepatocellular carcinoma involves promyelocytic leukemia protein and TRAIL independently of p53. Cancer Res 69:855–862.

Ho KK, McGuire VA, Koo CY, Muir KW, de Olano N, Maifoshie E, Kelly DJ, McGovern UB, Monteiro LJ, Gomes AR, Nebreda AR, Campbell DG, Arthur JS, Lam EW. 2012. Phosphorylation of FOXO3a on Ser-7 by p38 promotes its nuclear localization in response to doxorubicin. J Biol Chem 287:1545–1555.

Hoogeboom D, Essers MAG, Polderman PE, Voets E, Smits LMM, Burgering BM. 2008. Interaction of FOXO with beta-catenin inhibits beta-catenin/T cell factor activity. J Biol Chem 283:9224–9230.

Hu MC, Lee DF, Xia W, Golfman LS, Ou-Yang F, Yang JY, Zou Y, Bao S, Hanada N, Saso H, Kobayashi R, Hung MC. 2004. IkappaB kinase promotes tumorigenesis through inhibition of forkhead FOXO3a. Cell 117:225–237.

Inamura K, Matsuzaki Y, Uematsu N, Honda A, Tanaka N, Uchida K. 2005. Rapid inhibition of MAPK signaling and antiproliferation effect via JAK/STAT signaling by interferon-alpha in hepatocellular carcinoma cell lines. Biochim Biophys Acta 1745:401–410.

Kasai K, Ushio A, Kasai Y, Sawara K, Miyamoto Y, Oikawa K, Kuroda H, Takikawa Y, Suzuki K. 2012. Therapeutic efficacy of combination therapy with intra-arterial 5-fluorouracil and systemic pegylated interferon α-2b for advanced hepatocellular carcinoma with portal venous invasion. Cancer 118:3302–3310.

Katayama T, Nakanishi K, Nishihara H, Kamiyama N, Nakagawa T, Kamiyama T, Iseki K, Tanaka S, Todo S. 2007. Type I interferon prolongs cell cycle progression via p21WAF1/CIP1 induction in human colon cancer cells. Int J Oncol 31:613–620.

Katoh M, Katoh M. 2004. Human FOX gene family (Review). Int J Oncol 25:1495–1500.

Kayagaki N, Yamaguchi N, Nakayama M, Eto H, Okumura K, Yagita H. 1999. Type I interferons (IFNs) regulate tumor necrosis factor-related apoptosis-inducing ligand (TRAIL) expression on human T cells: a novel mechanism for the antitumor effects of type I IFNs. J Exp Med 189:1451–1460.

Kim BK, Han KH, Ahn SH. 2011. Prevention of hepatocellular carcinoma in patients with chronic hepatitis B virus infection. Oncology 81:41–49.

Kwon IK, Wang R, Thangaraju M, Shuang H, Liu K, Dashwood R, Dulin N, Ganapathy V, Browning DD. 2010. PKG inhibits TCF signaling in colon cancer cells by blocking beta-catenin expression and activating FOXO4. Oncogene 29:3423–3434.

Legrand A, Vadrot N, Lardeux B, Bringuier AF, Guillot R, Feldmann G. 2004. Study of the effects of interferon a on several human hepatoma cell lines: analysis of the signalling pathway of the cytokine and of its effects on apoptosis and cell proliferation. Liver Int 24:149–160.

Li C, Chi S, He N, Zhang X, Guicherit O, Wagner R, Tyring S, Xie J. 2004. IFNalpha induces Fas expression and apoptosis in hedgehog pathway activated BCC cells through inhibiting Ras-Erk signaling. Oncogene 23:1608–1617.

Lowry OH, Rosebrough NJ, Farr AL, Randall RJ. 1951. Protein measurement with the Folin phenol reagent. J Biol Chem 193:265–275.

Maiese K, Chong ZZ, Shang YC, Hou J. 2009. A ''FOXO'' in sight: targeting Foxo proteins from conception to cancer. Med Res Rev 29:395–418.

Medema RH, Kops GJ, Bos JL, Burgering BM. 2000. AFX-like Forkhead transcription factors mediate cell-cycle regulation by Ras and PKB through p27kip1. Nature 404:782–787.

Modur V, Nagarajan R, Evers BM, Milbrandt J. 2002. FOXO proteins regulate tumor necrosis factor-related apoptosis inducing ligand expression. Implications for PTEN mutation in prostate cancer. J Biol Chem 277:47928–47937.

Moro A, Santos A, Araña MJ, Perea SE. 2000. Activation of the human p27(Kip1) promoter by IFNalpha 2b. Biochem Biophys Res Commun 269:31–34.

Papageorgiou A, Dinney CP, McConkey DJ. 2007. Interferon-alpha induces TRAIL expression and cell death via an IRF-1-dependent mechanism in human bladder cancer cells. Cancer Biol Ther 6:872–879.

Pfeffer LM. 1997. Biologic activities of natural and synthetic type I interferons. Semin Oncol 24:S9-63–S9-69.

Quiroga AD, de Lujan Alvarez M, Parody JP, Ronco MT, Carnovale CE, Carrillo MC. 2009. Interferon-alpha2b (IFN-alpha2b)-induced apoptosis is mediated by p38 MAPK in hepatocytes from rat preneoplastic liver via activation of NADPH oxidase. Growth Factors 27:214–227.

Rozen S, Skaletsky H. 2000. Primer3 on the WWW for general users and for biologist programmers. Methods Mol Biol 132:365–386.

Sakae M, Kubo S, Takemura S, Sakata C, Uenishi T, Kodai S, Shinkawa H, Urata Y, Ohata K, Kaneda K, Nishioka T, Nozawa A, Suehiro S. 2012. Effect of interferon therapy on first and second recurrence after resection of hepatitis C virus-related hepatocellular carcinoma. Hepatol Res 42:564–573.

Schmittgen TD, Livak KJ. 2008. Analyzing real-time PCR data by the comparative C(T) method. Nat Protoc 3:1101–1108.

Seoane J, Le HV, Shen L, Anderson SA, Massagué J. 2004. Integration of Smad and forkhead pathways in the control of neuroepithelial and glioblastoma cell proliferation. Cell 117: 211–223.

Shen YC, Hsu C, Chen LT, Cheng CC, Hu FC, Cheng AL. 2010. Adjuvant interferon therapy after curative therapy for hepatocellular carcinoma (HCC): a meta-regression approach. J Hepatol 52:889–894.

Takeyasu M, Akuta N, Suzuki F, Seko Y, Kawamura Y, Sezaki H, Suzuki Y, Hosaka T, Kobayashi M, Kobayashi M, Arase Y, Ikeda K, Kumada H. 2012. Long-term interferon monotherapy reduces the risk of HCV-associated hepatocellular carcinoma. J Med Virol 84:1199–1207.

Toyoshima H, Hunter T. 1994. p27, a novel inhibitor of G1 cyclin-Cdk protein kinase activity, is related to p21. Cell 78:67–74.

Tsai WB, Chung YM, Zou Y, Park SH, Xu Z, Nakayama K, Lin SH, Hu MC. 2010. Inhibition of FOXO3 tumor suppressor function by betaTrCP1 through ubiquitin-mediated degradation in a tumor mouse model. PLoS One 5:e11171.

Wiley SR, Schooley K, Smolak PJ, Din WS, Huang CP, Nicholl JK, Sutherland GR, Smith TD, Rauch C, Smith CA, Goodwin RG. 1995. Identification and characterization of a new member of the TNF family that induces apoptosis. Immunity 3:673–682.

Yanase N, Hayashida M, Kanetaka-Naka Y, Hoshika A, Mizuguchi J. 2012. PKC-δ mediates interferon-α-induced apoptosis through c-Jun NH_2-terminal kinase activation. BMC Cell Biol 13:7.

Yang JY, Hung MC. 2011. Deciphering the role of forkhead transcription factors in cancer therapy. Curr Drug Targets 12:1284–1290.

Yang JY, Zong CS, Xia W, Yamaguchi H, Ding Q, Xie X, Lang JY, Lai CC, Chang CJ, Huang WC, Huang H, Kuo HP, Lee DF, Li LY, Lien HC, Cheng X, Chang KJ, Hsiao CD, Tsai FJ, Tsai CH, Sahin AA, Muller WJ, Mills GB, Yu D, Hortobagyi GN, Hung MC. 2008. ERK promotes tumorigenesis by inhibiting FOXO3a via MDM2-mediated degradation. Nature Cell Biol 10:138–148.

Yuan B, Latek R, Hossbach M, Tuschl T, Lewitter F. 2004. siRNA selection server: an automated siRNA oligonucleotide prediction server. Nucleic Acids Res 32:W130–W134.

Zhao LJ, Hua X, He SF, Ren H, Qi ZT. 2011. Interferon alpha regulates MAPK and STAT1 pathways in human hepatoma cells. Virol J 8:157.

Zhou Y, Wang S, Gobl A, Oberg K. 1999. Inhibition of CDK2, CDK4 and cyclin E and increased expression of p27Kip1 during treatment with interferon-alpha in carcinoid tumor cells. J Biol Regul Homeost Agents 13:207–215.

Zhou Z, Hamming OJ, Ank N, Paludan SR, Nielsen AL, Hartmann R. 2007. Type III interferon (IFN) induces a type I IFN-like response in a restricted subset of cells through signaling pathways involving both the Jak-STAT pathway and the mitogen-activated protein kinases. J Virol 81:7749–7758.

Address correspondence to:
María Cristina Carrillo
Instituto de Fisiología Experimental
Consejo Nacional de Investigaciones
Científicas y Técnicas (CONICET)
Facultad de Ciencias Bioquímicas y Farmacéuticas
Suipacha 570
Rosario 2000
Argentina

E-mail: carrillo@ifise-conicet.gov.ar

Received 7 November 2013/Accepted 10 April 2014

AUTHOR QUERY FOR JIR-2013-0124-VER9-CEBALLOS_1P

AU1: Please note that gene symbols in any article should be formatted per the gene nomenclature. Thus, please make sure that gene symbols, if any in this article, are italicized.

AU2: Please review all authors' surnames for accurate indexing citations. Please confirm all double surnames.